Monodisperse Hollow Supraparticles via Selective Oxidation

*Yunsheng Xia and Zhiyong Tang**

A novel and general strategy to fabricate monodisperse hollow supraparticles (SPs) via selective chemical oxidation is developed. Core-shell SPs made of semiconductor nanocrystals (NCs) are first obtained by an in situ assembly method. Subsequently, the cores can be selectively removed by preferential oxidation with dilute H_2O_2, resulting in formation of monodisperse hollow SPs. The structural parameters of the products, such as size, shell thickness, and composition, are tailored easily. The hollow structures achieved from CdSe/CdS core-shell SPs possess high fluorescence quantum yields and a large Stokes shift, the latter is remarkably different from that of conventional organic dyes and quantum dots. In addition to simple hollow structures, rattle-type nanostructures composed of semiconductor SPs or noble metal-semiconductor hybrids are also prepared, exemplifying the versatility of the proposed strategy.

1. Introduction

Nanomaterials with well-defined morphologies are of significant interest from fundamental research to technical applications because of their novel optical, electrical, magnetic and catalytic properties.[1,2] Among those materials with distinct structural and geometrical characteristics, hollow nanostructures have received considerable attention recently due to their many applications in confined-space chemical reaction, catalysis, controlled delivery, biomedical sensing and diagnosis, etc.[3–8] Until now, hollow nanostructures of various compounds have been fabricated by different synthetic approaches. Generally, there are three methods, namely kirkendall effect,[9,10] Ostwald ripening[11–13] and galvanic replacement,[14,15] to be used for preparation of hollow nanostructures with crystalline materials. Unfortunately, all the three methods have application limitations. For example, kirkendall effect often takes effect at the elevated temperature to accelerate the outward diffusion of substances from the cores,[9] and its exact process need be further elucidated.[4] Ostwald ripening is suitable for synthesis of hollow metal oxide structures with considerably large sizes (several hundred nanometers),[12] while galvanic replacement is only applied for noble metal nanoparticles (NPs). So, it is highly desirable to explore new strategies for fabrication of hollow nanostructures, especially semiconductor materials or semiconductor-based hybrids with unique optical/electrical properties.

Alternatively, chemical etching is a versatile and reliable method for fabrication of hollow nano-/micro- structures via selective removal of the cores from the preformed core/shell structure, which is based on the difference in chemical stability of the core and shell materials. However, the precondition of chemical etching method is requirement of noncrystalline or amorphous shells,[5,16] because, differently from the crystalline shells, the amorphous coating facilitates the entrance of etching agents (small molecules or ions) and thus benefits selective removal of the cores. As a result, the majority of the hollow nanostructures produced by chemical etching are amorphous silica that lacks interesting optical/electrical properties.

Herein, we suggest that a new type of core-shell nanostructures composed of supraparticles (SPs) can be good candidates for fabrication of hollow materials.[17] Compared with conventional single crystalline or polycrystalline core-shell nanostructures, the etching agent, dilute H_2O_2, easily diffuses into the interior of SPs due to many grain boundaries among individual NP units in the shells. Therefore, the cores of SPs are selectively removed by preferential oxidization with dilute H_2O_2, resulting in formation of hollow SPs with controllable sizes, shell thicknesses and compositions. Impressively, in addition to simple hollow structures, this method is applicable for synthesis of rattle-type nanostructures with either semiconductor or noble metal cores. It is noted that all the hollow SPs exhibit specific and tunable optical properties, which are different from conventional dye molecules or quantum dots.

2. Results and Discussion

2.1. Monodisperse Core-Shell SPs

Monodisperse SPs are prepared by in-situ assembly method that we developed recently.[17] **Figure 1**A,B represent typical SEM and TEM images of CdSe SP cores obtained by directly

Prof. Y. Xia
College of Chemistry and Materials Science
Anhui Normal University
Wuhu, 241000, China
Prof. Z. Tang
Laboratory for Nanomaterials
National Center for Nanoscience and Technology
Beijing, 100190, China
E-mail: zytang@nanoctr.cn

DOI: 10.1002/adfm.201200311

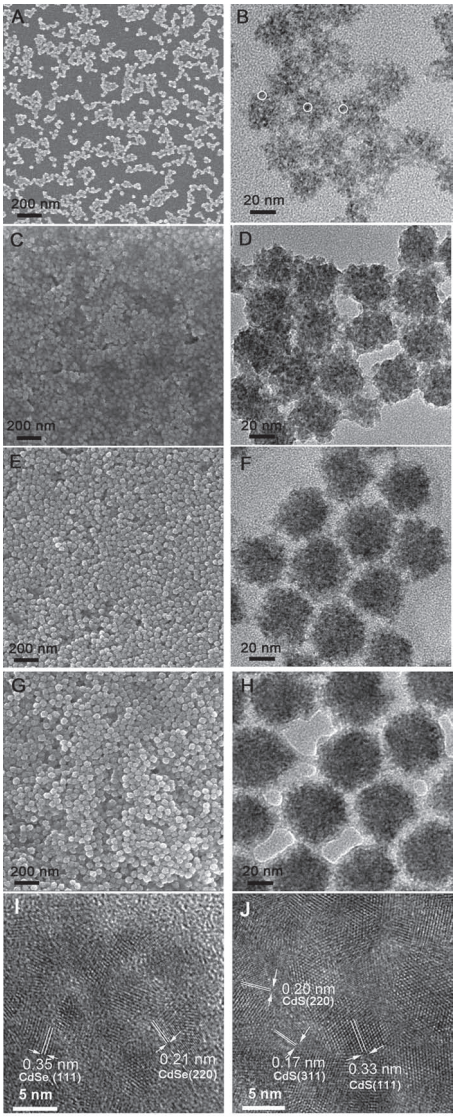

Figure 1. SEM and TEM images of CdSe SP cores with the diameters of 34.2 nm (A,B). SEM and TEM images of CdSe/CdS core-shell SPs with the diameters of 39.4 nm (C,D) (referred to as CdSe/CdS-40), 44.4 nm (E,F) (referred to as CdSe/CdS-44), and 49.7 nm (G,H) (referred to as CdSe/CdS-50). HRTEM images of CdSe SP cores (I) and CdSe/CdS-50 core-shell SPs (J).

heating the precursor solution at 90 °C for 24 h. All CdSe SPs have uniform spherical shapes with the average diameter of about 34.2 nm, in which individual CdSe nanocrystals (NCs) are clearly discerned (white circles in Figure 1B). HRTEM image (Figure 1I) further shows that the CdSe SPs are polycrystalline in structure, and the lattice plane spacings are measured to be 0.35 nm for (111) and 0.21 nm for (220), respectively, which are typical for zinc blende CdSe structures. The mean sizes of individual CdSe NCs inside the SPs are about 3.0 nm.

After addition of thioacetamide (the molecular ratio between S and Se precursors is 1:1) into the solution containing CdSe SPs and reacting for 24 h at 70 °C, the average size of the SPs increases from 34.2 to 39.4 nm (Figure 1C,D). As comparison, CdSe SPs keep their size almost invariable under the same experimental conditions in absence of thioacetamide (not shown). Therefore, increase in the size of SPs should result from coating of CdS layer around CdSe SPs. Moreover, as the concentrations of thioacetamide are gradually increased (the molecular ratios between S and Se precursors are changed to 2.3:1 and 4.0:1, respectively, meanwhile Cd^{2+} concentration remains always excessive), the size of SPs correspondingly increases to 44.4 nm (Figure 1E,F) and 49.7 nm (Figure 1G,H). According to their diameters, the three types of core-shell SPs are named as CdSe/CdS-40, CdSe/CdS-44 and CdSe/CdS-50, respectively. It should be pointed out that S precursors, thioacetamide, are added in the solution of CdSe SP cores step by step in order to avoid possible assembly of CdS itself and accurately tune the thickness of CdS shells. Both SEM (Figure 1C,E,G) and TEM (Figure 1D,F,H) images reveal that all the products are monodisperse SPs, and no small SPs and separate NCs are found. These results indicate that the capping processes are effective and uniform. As shown in Figure 1J, three different lattice plane spacing are observed in the HRTEM image of CdSe/CdS-50, and their values are 0.33, 0.20 and 0.17 nm, corresponding to the (111), (220) and (311) planes of zinc blende CdS, respectively. The average size of individual CdS NCs in the shells is about 3.0-5.0 nm. All the above results definitely indicate that CdSe SP cores are capped by CdS NCs to form core-shell SPs. The thicknesses of CdS layers for CdSe/CdS-40, CdSe/CdS-44 and CdSe/CdS-50 are calculated from TEM images to be 2.6, 5.1 and 7.8 nm, respectively. Interestingly, we notice that the monodispersity of the SPs is improved with CdS coating. As shown in Table S1, the size distribution of CdSe SP cores is 12.0%, as determined by TEM. After CdS coating, the dispersity of CdSe/CdS-50 samples is decreased to 7.7%. The reason might be ascribed to the fact that small SP cores containing less CdSe NCs have weak Coulomb repulsion for exterior NCs, which preferentially attach CdS layers compared with large SPs.[17] In addition, the average sizes of CdSe cores and three CdSe/CdS core-shell SPs are measured by DLS technique to be 42.7, 49.4, 55.3 and 59.9 nm, respectively (Figure S1, Supporting Information).The values obtained by DLS technique are the hydrodynamic diameters of particles, which are larger than the values obtained by TEM imaging due to presence of a hydration layer and the stronger scattering of larger particles.[18] Nevertheless, DLS results confirm that all assembly processes take place in solution rather than on the substrates during drying.

The core-shell structures of CdSe/CdS SPs are directly disclosed by EDX elemental mapping and line scan. **Figure 2** shows the HAADF-STEM image of CdSe/CdS-50 and corresponding EDX elemental mapping of S, Se, and Cd, which can give us some straightforward information on the structure of the as-prepared SPs. First, Se element (Figure 2D) is located at the center of each SP, and its area is obviously smaller than that of S (Figure 2C) and Cd (Figure 2B). Second, more S element is located at the periphery of the SPs in respect to the center position (Figure 2C). Lastly, the profile of Cd element is coincident with that of S, but its distribution is uniform on the whole SPs (Figure 2B). Altogether, Figure 2 gives us a doubtless proof for formation of CdSe/CdS core-shell nanostructures. Based on Figure 2B–D, the thickness of the CdS layer for CdSe/CdS-50 is

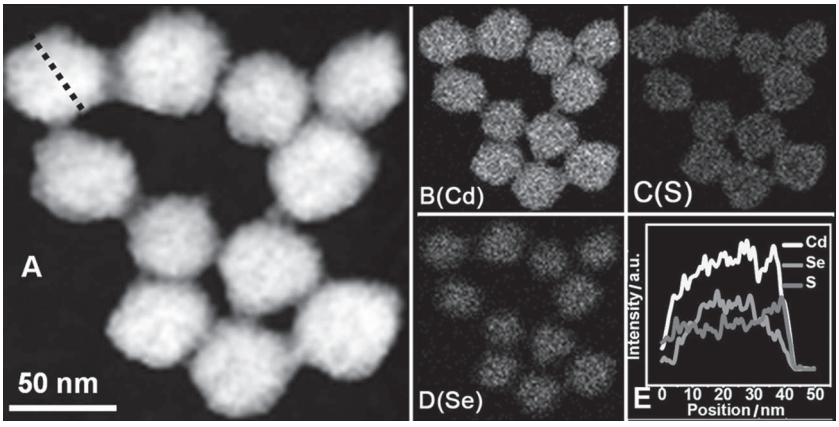

Figure 2. HAADF-STEM image of CdSe/CdS-50 (A), and corresponding EDX mapping of Cd (B), S (C), and Se (D). Line scan of CdSe/CdS-50 (E).

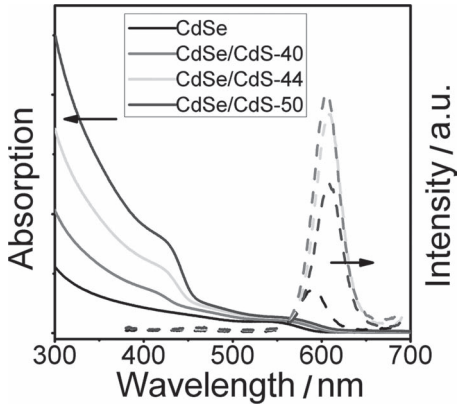

Figure 3. UV-Vis (solid curves) and fluorescence (dashed curves) spectra of CdSe and CdSe/CdS SPs with different shell thicknesses.

estimated to be about 5.1 nm, which is slightly smaller than that obtained by TEM imaging. The reason should arise from mutual penetration of CdSe and CdS NCs at their interface, since the edge of CdSe SP cores is rather rough (Figure 1A). In addition to core-shell structure, EDX line scan also proves the interpenetration of CdSe into the CdS at the interface of the products (Figure 2E).

The gradual coating processes can be in-situ monitored by both UV-Vis and fluorescence spectra (**Figure 3**). CdSe SP cores have an obvious absorption shoulder at 547 nm (the first solid curve from bottom), so the average size of CdSe NCs within SPs are calculated to be 3.0 nm by empirical equations,[19] which is in good agreement with the value estimated from TEM imaging. It is evident that the CdSe SPs exhibit quantum confinement effect similar to that of single CdSe NCs. The CdSe SPs show rather weak fluorescence with a peak located at 589 nm (the dashed curve from bottom), and the fluorescence quantum yields (QYs) are below 0.2%. Once the CdSe SP cores are capped by CdS shells, the first absorption peak of the CdSe/CdS-40 products shows a little red shift and a new absorption shoulder appears at 400–450 nm (the second solid curve from bottom). Simultaneously, the fluorescence peak shifts from 589 to 606 nm with an obvious intensity enhancement (the first dashed curve from top). The bathochromic shifts of both absorption and fluorescence peaks originate from delocalization of the electron and hole wave functions of the CdSe cores into the CdS shells, which are similar with those of conventional CdSe/CdS core-shell quantum dots.[20] The new absorption characteristic at 400–450 nm is assigned to formation of the CdS shells, while the fluorescence enhancement of the SPs after coating is also attributed to the passivation effect of the CdS shells. As the SPs are capped in succession by the CdS shells, the peak positions of both the first absorption and fluorescence of the products have no obvious changes. However, the absorption intensity below 450 nm increases remarkably, indicating the increased thickness of the CdS shells around the SP cores.

2.2. Hollow SPs via Selective Oxidation of Core-Shell SPs

To obtain hollow nanostructures via selective etching of the core-shell SPs, H_2O_2 is selected as the etching agent due to the mild oxidation property and no additional side products except for H_2O.[21,22] **Figure 4**A represents UV-Vis spectra of the CdSe/CdS-50 solution via gradual oxidization by H_2O_2. Notably, the absorption shoulders at 550–600 nm belonging to CdSe cores show continuous blue shifts with an obvious decrease in their intensities, eventually leading to almost disappearance of the absorption features. As comparison, the absorption characteristics of CdS at 400–450 nm keep always distinct in whole oxidization processes. We also notice that the intensity at shorter wavelength, 400–450 nm, decreases with gradual oxidation. Such a decrease of absorption intensity is mainly assigned to the oxidation of CdSe, because the absorption band of CdSe NCs is very broad and extends to UV region. Based on evolution

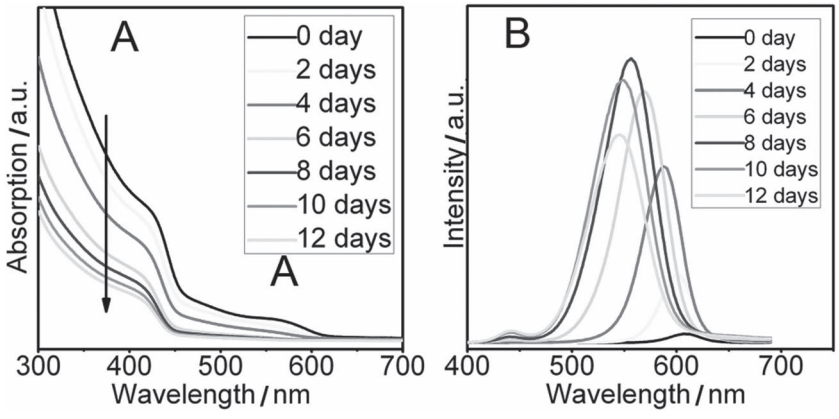

Figure 4. UV-vis and fluorescence spectra of CdSe/CdS-50 with different oxidation times.

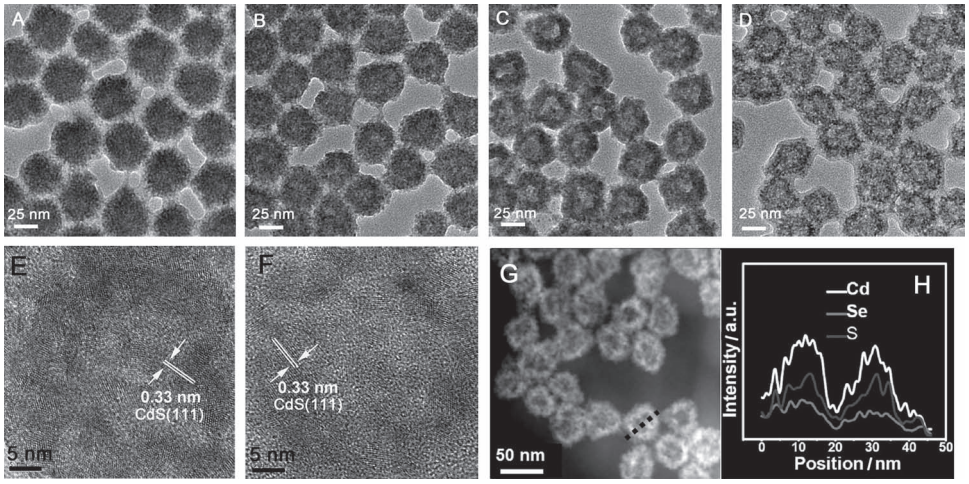

Figure 5. TEM images of CdSe/CdS-50 with different oxidation time before etching (A), etching for 4 days (B), 8 days (C,E), and 12 days (D,F). E,F) Show HRTEM images of (C,D), respectively. HAADF-STEM image of CdSe/CdS-50 after etching for 12 days (G). EDX line-scan profiles (H) of single SP in (G).

of absorption spectra, we can conclude that CdSe cores in the core-shell SPs are preferentially oxidized. Such selective etching of CdSe cores is in contradiction to the previous report on monodisperse CdSe/ZnS core-shell quantum dots or CdSe/ZnS/CdSe core-shell-shell quantum dots, in which the etching processes were found to proceed from outside to inside and stopped immediately once the outer layer could not be oxidized.[23]

To further clarify the oxidization behavior of the core-shell SPs, TEM and corresponding EDX are used to study the evolutionary changes of the nanostructures with different oxidation time (**Figure 5**). Before oxidation, the CdSe/CdS core-shell SPs appear uniform for the whole particles because CdSe and CdS have similar contrast. After oxidized for 4 days, the contrast at the central part of each SP becomes weak (Figure 5B), indicating formation of hollow structures. This observation is consistent with the result of UV-Vis absorption spectra, in which the central CdSe cores are found to be preferentially etched (Figure 4A). Generally, the oxidation product of CdSe is $CdSeO_3$ instead of CdO,[24] because the latter is unstable especially in aqueous solution.[25] Differently from observation on the etching behavior of oleic acid capped CdSe quantum dots,[26,27] we did not find white precipitate of $CdSeO_3$ during oxidation of CdSe/CdS SPs. The possible reason is the strong coordination effect of largely excessive citrate stabilizers for Cd^{2+} ions, which effectively prevents formation of $CdSeO_3$ precipitates. As expected, etching with longer time can remove more CdSe cores, meanwhile generating dissolved Cd complexes and SeO_3 anions in solution. As shown in Figure 5C,D, the thicknesses of the CdS shells are correspondingly shrunk to 12–15 nm and 7–9 nm after etching for 8 and 12 days, respectively, while the average diameter and size distribution of the hollow structures remain 46 nm and 7.7%, respectively. HRTEM and SEM images confirm that the CdS NCs in the shells keep relatively intact (Figure 5E,F, and Figure S2 (Supporting Information)), which is consistent with the result of UV-Vis absorption spectra (Figure 4A). The EDX line-scan profiles of single SP via etching for 12 days are shown in Figure 5H, which gives us a distinct proof for formation of the hollow structures. Figure 5H also demonstrates that not all the Se element near the shells can be removed even after etching for 12 days, which is reasonable considering that interpenetration of CdS and CdSe may effectively protect CdSe at the interface from etching.

Preferential oxidation of CdSe is easily to be understood because the reducibility of Se^{2-} (–0.92 V) is stronger than that of S^{2-} (–0.48 V). The only raised question is why outer CdS layer cannot prevent oxidation of inside CdSe cores, just as the previously-reported CdSe/ZnS core-shell quantum dots?[21] To directly compare the difference of the oxidization behaviors, we also synthesized conventional CdSe/CdS core-shell quantum dots for control experiments. For CdSe/CdS core-shell quantum dots, the absorption characteristics of CdSe (550–600 nm) keep almost invariable and CdS absorption intensities (<450 nm) show obvious decrease after oxidation for 3 days; while for CdSe/CdS core-shell SPs, the absorption peaks of CdSe exhibit evident blue shifts and the peak intensities decrease under the same oxidative conditions (Figure S3, Supporting Information). These control experiments clearly demonstrate that oxidation of conventional core-shell quantum dots starts from the outside CdS shells rather than easily-oxidized CdSe cores. The difference in the oxidation behaviors results from the difference in the structures. The shells of conventional core-shell quantum dots are complete with single crystalline or polycrystalline structures, in which no interstice exists. So the oxidation process has to go on from outside to inside, or stop immediately if the outer layer cannot be oxidized. For core-shell SPs, the CdS shells are formed via assembly of small CdS NCs and there are many spaces between NC building blocks (Figure 1). Thus, small molecules, such as H_2O_2, easily diffuse into the CdSe cores of SPs along their grain boundaries. Furthermore, our recent study reveals that the packing density of CdSe NCs in the cores is nonuniform and it increases from the center to the edge because of the larger Coulomb repulsion in the center.[17] This unique structure gives rise to oxidation starting from the loosely packed centers of the cores (Figure 4 and **Scheme 1**).

The prepared hollow SPs show unique fluorescence properties. Figure 4B presents the fluorescence spectra of CdSe/CdS-50

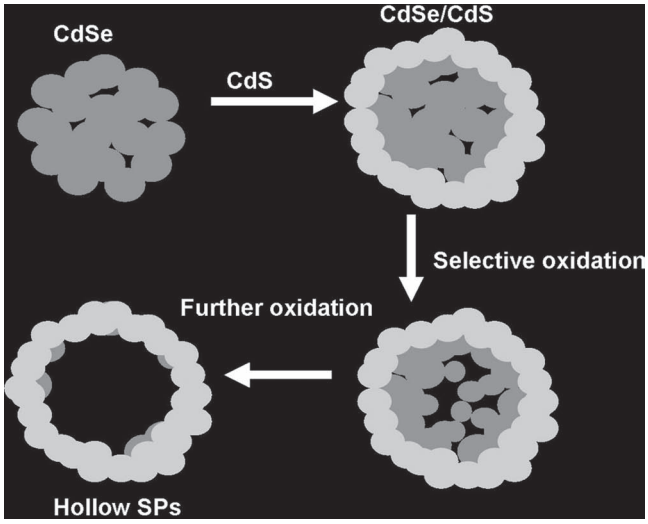

Scheme 1. Formation process of hollow SPs.

with different oxidation time. The fluorescence peaks of CdSe/CdS-50 exhibit monotonous blue shifts during oxidation due to the continuous decrease of CdSe sizes. On the other hand, the change of the fluorescence intensity is complex. At the early stage, the fluorescence intensity increases with the oxidization time prolonging, and the fluorescence QY of the hollow SPs gets up to the maximum 44% after 8 days. Subsequently, the fluorescence intensity becomes decreasing. Because of the high QY and narrow full width at the half peak height (30–50 nm, dependent on the oxidization time), such fluorescence should originate from the CdSe cores instead of surface state recombination of the CdS shells. Up to now, although a few CdS- and other semiconductor- based hollow structures had been synthesized based on different mechanisms,[28–30] their optical properties, especially fluorescence QYs, have never been mentioned. Herein, the unusually high QY of the hollow SP structures is mainly ascribed to three reasons. First of all, the prepared products possess well-defined nanostructures. The cores and shells are respectively composed of several nanometer sized CdSe NCs and CdS NCs with obvious quantum confinement effect, which provide the potential of excellent optical properties. Also, CdSe NCs in the cores are capped by CdS NCs in the shells, which makes the CdSe surface passivated just like that of conventional CdSe/CdS core-shell quantum dots.[20] Second, the mild oxidization is employed in the experiments. As-prepared SPs have very low QY (<1%) before oxidization due to the fact that there are large numbers of traps on the CdSe NC surface synthesized at rather low reaction temperature (<100 °C). After they are oxidized by dilute H_2O_2 with natural light, the surface traps are effectively removed, leading to strong fluorescence. Similar oxidation-induced enhancement of CdSe NC fluorescence has been discussed in the literatures.[26,27,31] Lastly, the effect of fluorescence resonance energy transfer (FRET) in SPs might enhance the CdSe emission. When two quantum systems are close to each other within the distance of less than 10 nm, FRET process will happen if their optical bands are well overlapped.[32] Herein, many CdS NCs in the shells have strong absorbance at the short wavelength, and the corresponding energy at the excitation state can be effectively transferred to the adjacent CdSe NC cores via the FRET process, considering that the broad absorbance of CdSe NCs overlaps the emission of CdS shells. The fluorescence spectra also give us some information about occurrence of FRET. In the beginning, there is only one fluorescence peak from CdSe NCs. However, an additional peak appears at 442 nm (from CdS NCs) after 8 days oxidation. The intensity of the fluorescence peak at 442 nm increases with the oxidization time prolonging. The reason for appearance of the fluorescence peak at 442 nm and its changes in intensity could be interpreted by the FRET effect. At first, emission of CdS NCs in the shells is effectively quenched because of FRET from CdS to CdSe. However, as more and more CdSe NCs in the cores are etched, the residual CdSe NCs cannot "accept" whole energy from CdS NCs. So, some excessive energy of CdS NCs at the excitation state is relaxed through radiative recombination (fluorescence). It should be stressed that thanks to FRET occurrence, the fluorescence of the hollow SPs displays very large Stokes shift (>100 nm, as shown in Figure 4), which is remarkably different from that of conventional organic dyes and quantum dots.[19,20,32,33] Therefore, such specific optical properties make the monodisperse hollow SPs have potential applications in biology and photonic crystals. We also notice that both the positions and intensities of the fluorescence peaks of the hollow structures become relatively stable after oxidation for 8 days, which might result from the fact that CdSe at the interface is protected by CdS due to interpenetration. This hypothesis can be supported by structural analysis from TEM imaging and the corresponding line scan (Figure 2).

The optical photographs record the color and fluorescence changes of CdSe/CdS-50 solution with different oxidization time (**Figure 6**). The solution keeps transparent all the time, and its color varies from orange to green because of gradual decrease of the amount ratio of CdSe to CdS. Under UV light, the SP solution shows strong fluorescence after oxidation, and its emission color is easily modulated from red to green just by controlling the oxidation time.

Lastly, the structural parameters of the hollow SPs could be easily tailored by altering the experimental conditions. For example, the shell thickness can be tuned by the degree of oxidation degree or the thickness of pre-coating CdS layer. The shell thickness of the hollow nanostructure is about 12–15 nm (Figure 5C,F) after oxidation for 8 days and 7–9 nm

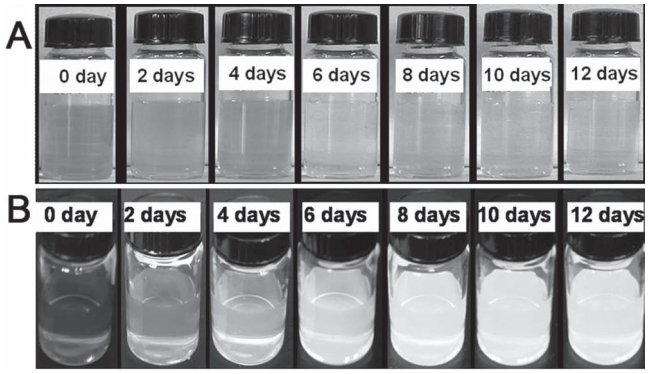

Figure 6. Photographs of CdSe/CdS-50 solution under room lighting (top) and UV light (bottom) with different oxidation times.

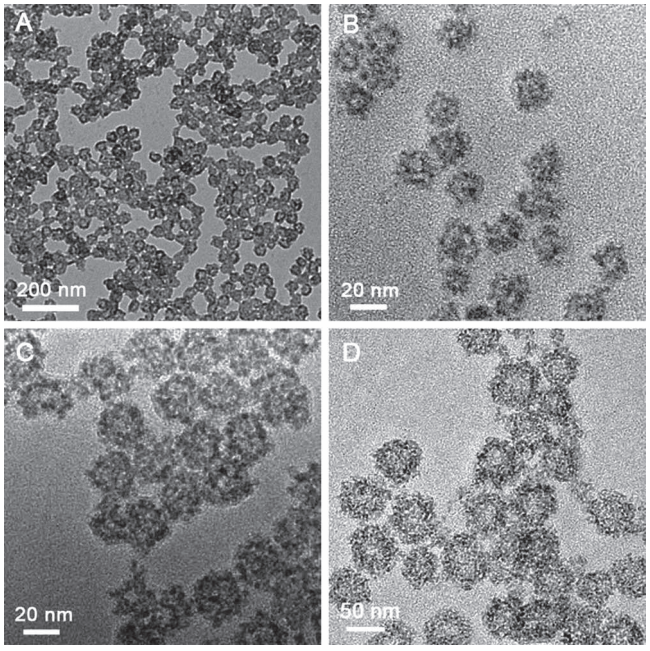

Figure 7. TEM images of hollow SPs with different parameters. Hollow CdS SPs with shell thickness of 5-7 nm from CdSe/CdS-44 (A), CdSe/CdS-19 (B), and CdSe/CdS-26 (C). ZnS hollow SPs from ZnSe/ZnS (D). The overall sizes of the samples in panels (A, B, C, and D) are 42, 18, 24, and 54 nm, respectively, while the corresponding size distributions are 8.4%, 9.5%, 7.6%, and 10.5%, respectively.

after oxidation for 12 days (Figure 5D,F). It is notable that the mild etching reaction can be stopped at any time by removing H_2O_2 using sodium sulfite. Similarly, hollow SPs with thinner CdS shell (only 5–7 nm) as shown in **Figure 7**A can be obtained while oxidizing CdSe/CdS-44. Except for the shell thickness, the size of the hollow SPs could also be tuned by changing the size of the CdSe NC cores. For example, as shown in Figure 7B,C, hollow CdS SPs with the diameters of 18 nm and 24 nm can be obtained by smaller CdSe/CdS SPs as templates, respectively. It is noted that the diameters of hollow SP products are slightly smaller than those of the mother templates (19 nm and 26 nm). A plausible explanation is that there are many voids between CdS NCs in the shell, so the shrinkage of the SPs occurs as the inner layer is etched away. In addition to hollow CdS SPs, the present approach could easily extend to other types of semiconductor materials. As an example, Figure 7D presents hollow ZnS SPs obtained from ZnSe/ZnS SPs (Figure S4 and S5, Supporting Information) by the identical oxidization process. In principle, any types of hollow SPs can be obtained by this strategy as long as the cores and shells of SPs exhibit difference in the oxidation-reduction potentials.

Besides the tunable parameters of the hollow products, we have found that other oxidation agent also gives rise to a similar hollow structure. As shown in Figure S6 (Supporting Information), CdSe/CdS core/shell SPs turn from solid to hollow by bubbling oxygen for 7 days. The result demonstrates that the selective oxidation method is versatile for synthesizing hollow structures.

2.3. Rattle-Type SPs via Selective Oxidation of Core-Shell-Shell SPs

Rattle-type (core in hollow) nanoparticles have recently attracted much interest because of potential applications in many fields arising from their specific structure.[34–41] Since selective oxidation of SPs is versatile, we hope to extend this method to fabrication of rattle-type SPs. Firstly, CdS/CdSe/CdS core-shell-shell SPs are constructed, and their well-defined structures are resolved by TEM and the corresponding elemental mapping (Figures S7 and S8).

The synthesized core-shell-shell SPs are treated by dilute H_2O_2. As expected, the middle layer (CdSe) is oxidized preferentially (**Figure 8**A). The SPs have a discernable rattle-type structure after oxidation for 6 days (Figure 8B,E), and further oxidation produce larger spaces between CdS cores and shells (Figure 8C,D,F). As far as we know, rattle-type nanostructures that both cores and shells are fully assembled by NCs have not been reported yet. Similar to hollow CdS SPs, the monodisperse rattle-type SPs also exhibit strong and tunable fluorescence, and the maximum QY gets up to around 25% (Figure S11 and S12, Supporting Information).

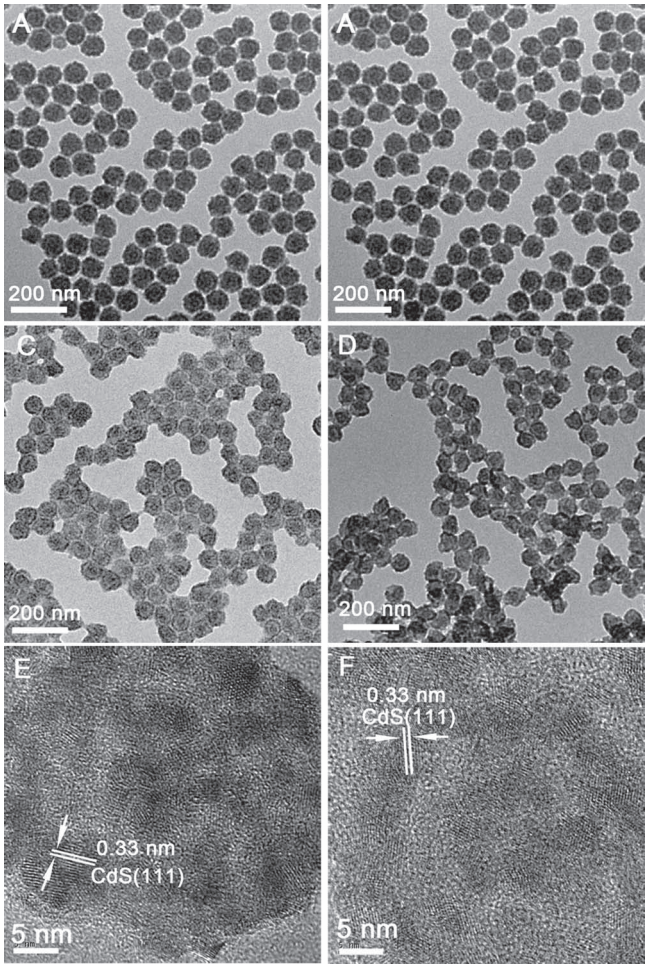

Figure 8. TEM and HRTEM images of CdS/CdSe/CdS SPs with different oxidization time: A) 3 days, B,E) 6 days, C,F) 9 days, and D) 12 days. Panels (E,F) show HRTEM images of (B,C), respectively. The overall sizes and size derivation of the samples in (A–D) remain about 52 nm and 5.8%.

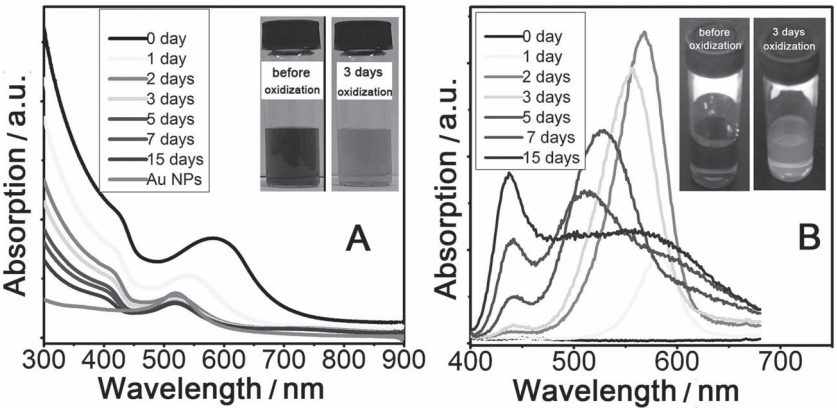

Figure 9. A) UV-vis and B) fluorescence spectra of Au/CdSe/CdS SPs with different oxidation time. Photographs of Au/CdSe/CdS SPs before and after oxidation for 3 days under room lighting (insets of (A)) and UV light (insets of (B)).

Besides semiconductor materials, we could also obtain the hybrid rattle-type SPs composed of gold cores and CdS shells. To achieve such a structure, Au/CdSe/CdS core-shell-shell SPs are firstly synthesized (Figure S13, Supporting Information). HAADF-STEM image (Figure S14, Supporting Information) demonstrates that Au/CdSe/CdS structure is formed indeed. As shown in Figure S15B (Supporting Information), the surface plasmon resonance (SPR) absorption of Au NPs increases gradually and shifts from 520 to 605 nm after growth of 18 nm thick CdSe (CdS) shell. Such a SPR red-shift is consistent with the theoretical calculation result.[42] As the Au/CdSe/CdS SPs are oxidized by H_2O_2, their SPR absorption decreases and shifts to the short wavelength dramatically. It returns to 520 nm after two days and maintains unchanged for further oxidation (**Figure 9**A). At the same time, the solid core-shell-shell SPs changed to uniform rattle-type structures containing Au cores and CdS shells after etching for 7 days (**Figure 10**A–C). Furthermore, the hollow space can be easily tuned by the oxidation time (Figure 10D–F).

The different hybrid systems composed of Au and CdS materials, such as matchstick, dumbbell and core/shell structures have been obtained, and their optical properties are depended on the exact hybrid structures.[43–45] In the present system, solid Au/CdSe/CdS SPs do not show any fluorescence because of many surface traps as well as the strong quenching of Au cores.[44] Interestingly, a visible fluorescence is observed for hybrid SPs after etching by dilute H_2O_2 (inset in Figure 9B), although the emission intensity is relatively weak (quantum yield is about 0.8%) as compared to that of other SPs (hollow CdS or rattle CdS/CdS nanostructures). The increased fluorescence of hybrid SPs could result from two reasons. Firstly, mild oxidation of H_2O_2 effectively decreases the surface traps of the particles, which is similar to that of above SPs. Secondly, removal of middle layer of CdSe weakens the quenching effect of Au cores, as considering that the distances between Au cores and some parts of CdS increase due to the movement of cores in the rattle structures. Recently, semiconductor NC/gold core-shell NPs with simultaneous fluorescence and surface plasmon resonance (SPR) properties are demonstrated.[46] In the present study, the SPs with a defined interior architecture also exhibit both fluorescence and SPR characteristics. This rattle noble metal-semiconductor hybrid nanostructure may offer a new and interesting platform for study of exciton-plasmon interactions.

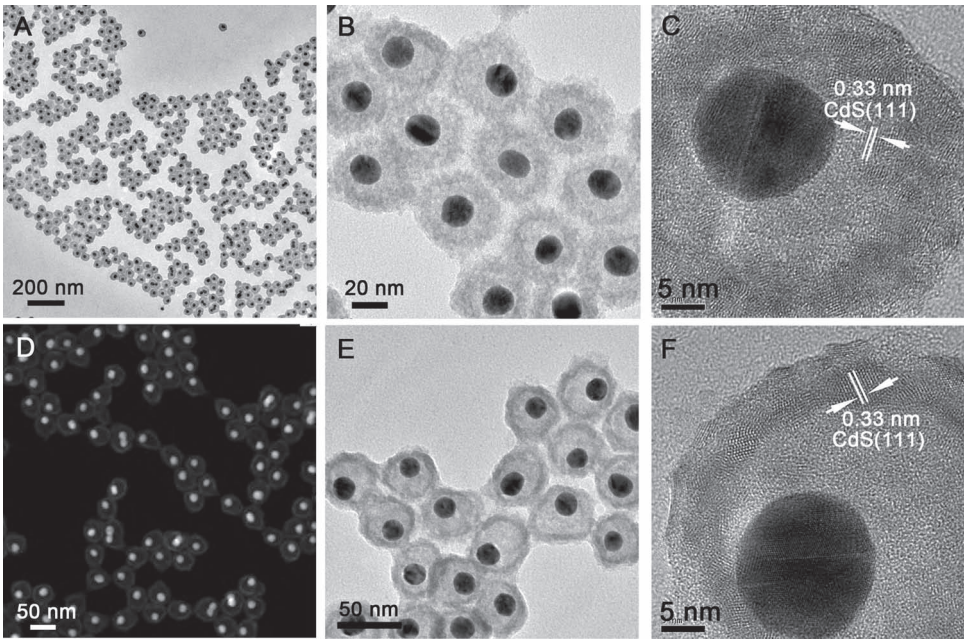

Figure 10. Rattle-type Au/CdS nanostructures after etching by dilute H_2O_2 for 7 days (A–C) and 15 days (D–F). The overall sizes and size derivation of the samples in (A–C) and (D–F) are 44 nm and 6.4%.

3. Conclusions

By combination of in-situ assembly and selective oxidization, simple hollow SPs or rattle-type SPs with narrow size distributions and high stability had been fabricated. The unique structures and formation processes endow the products with special optical properties. The results reported here highlight that the strategy combined self-assembly with rational chemical reaction is promising to accurately tailor both the structures and properties of hollow nanomaterials.

4. Experimental Section

Chemicals: $Cd(ClO_4)_2{\cdot}6H_2O$, $Zn(ClO_4)_2{\cdot}6H_2O$, sodium citrate dihydrate, thioacetamide, NaOH and $HAuCl_4{\cdot}3H_2O$ were purchased from Alfa Aesar. N,N-dimethylselenourea was obtained from Sigma-Aldrich. H_2O_2 was purchased from Guoyao Company, China. All chemicals were used as received. Milli-Q deionized water was used for all the experiments.

Characterizations: UV-Vis absorption (Hitachi U-3010) and fluorescence spectroscopy (Horiba Jobin Yvon FM-4) were conducted to record the optical properties of the products at room temperature. Morphologies of the products were observed by scanning electron microscopy (SEM, Hitachi S-4800, Japan) under the accelerating voltage of 10 kV. The samples for SEM characterization were all prepared by dropping the aqueous suspension of the SPs on clean silicon substrates and then being dried in air. Characterizations of transmission electron microscopy (TEM) were carried out on Tecnai G2 20 ST (FEI, America) under the accelerating voltage of 200 kV. Scanning transmission electron microscopy (STEM) and energy dispersive X-ray spectroscopy (EDX) investigations were performed in G2 F20 U-TWIN (FEI, America) using a high-angle annular dark field (HAADF) detector. High-resolution TEM (HRTEM) was also performed using a G2 F20 U-TWIN TEM operating at 200 kV. SP dispersions in solution were analyzed for mean particle diameter sizes using dynamic light scattering (DLS, Zetasizer Nano ZS series; Malvern Instruments) with 633 nm laser wavelength and a measurement angle of 173° (backscatter detection) at 25 °C. Before analysis, SP samples were filtered through a 0.2 μm filter.

Synthesis of Core-Shell SPs: All SPs were obtained based on the previous report with some modification.[17] We used synthesis of CdSe/CdS core-shell SPs with 34 nm cores as an example. Firstly, CdSe SPs were prepared as the cores by in-situ assembly through the following steps: (1) sodium citrate dehydrate (0.10 g) was dissolved in pure water (90 mL) in a 150 mL flask; (2) $Cd(ClO_4)_2{\cdot}6H_2O$ (0.0672 g) was added in the flask under stirring; (3) The pH of the mixed solution was adjusted to 9.0 by NaOH (0.4 M); (4) N,N-dimethylselenourea (0.003 g) was added into the 150 mL flask after the mixed solution were bubbled with argon for 15 min; (5) The prepared reaction solution was transferred to a 250 mL three-neck flask and heated to 90 °C in oil bath for 24 h under flowing argon for synthesis of CdSe SPs. After that, the obtained CdSe SP solution was cooled naturally to room temperature for growth of CdS shells onto CdSe SPs. Subsequently, thioacetamide (0.0015 g) was added into the cooled CdSe SP solution and then the solution was heated to 70 °C for 24 h under argon flow so that CdSe/CdS core-shell SPs were obtained. Note that the capping process could be repeated several times for controlling thickness of the shell.

For SPs composed of 19 nm CdSe cores, the processes were the same as those of 34 nm ones only except that 0.006g N,N-dimethylselenourea was added. For SPs composed of 14 nm CdSe SPs, the solution containing precursors was heated in a conventional 900-W microwave oven for 60 seconds. For ZnSe/ZnS core-shell SPs, $Cd(ClO_4)_2{\cdot}6H_2O$ was replaced by $Zn(ClO_4)_2{\cdot}6H_2O$, and oil bath heating was replaced by microwave heating for 30 min at 120 °C for synthesis of ZnSe SPs. CdS/CdSe/CdS and Au/CdSe/CdS core-shell-shell SPs were obtained by similar method except that two shell materials were added in sequence. Au nanoparticles were synthesized based on the previous report.[47]

Selective Oxidation of Core-Shell SPs: In a typical procedure, H_2O_2 (0.6%, 0.10 mL) was added every 24 h to the 12 mL CdSe/CdS SP solution. For hollow ZnS SPs, H_2O_2 (0.2%, 0.05 mL) was added every 24 h to the 12 mL ZnSe/ZnS SP solution. All solutions were placed under natural light, and aliquot solutions were taken at different time so as to monitor the oxidation process.

Supporting Information

Supporting Information is available from the Wiley Online Library or from the author.

Acknowledgements

The authors are grateful to financial support from National Natural Science Foundation for Distinguished Youth Scholars of China (21025310), National Natural Science Foundation of China (20973047, 20905002, 91027011), the National Research Fund for Fundamental Key Project (2009CB930401), China-Korea Joint Research Project (2010DFA51700), 100-Talent Program of Chinese Academy of Sciences, and the Knowledge Innovation Project of the Chinese Academy of Science (KJCX2-YW-M20).

Received: February 2, 2012
Revised: March 13, 2012
Published online: April 12, 2012

[1] C. Burda, X. Chen, R. Narayanan, M. A. El-Sayed, *Chem. Rev.* **2005**, *105*, 1025.
[2] Y. Jun, J. Choi, J. Cheon, *Angew. Chem. Int. Ed.* **2006**, *45*, 3414.
[3] J. Goldberger, R. Fan, P. Yang, *Acc. Chem. Res.* **2006**, *39*, 239.
[4] X. W. Lou, L. A. Archer, Z. Yang, *Adv. Mater.* **2008**, *20*, 3987.
[5] Q. Zhang, W. Wang, J. Goebl, Y. Yin, *Nano Today* **2009**, *4*, 494.
[6] J. Liu, F. Liu, K. Gao, J. Wu, D. Xue, *J. Mater. Chem.* **2009**, *19*, 6073.
[7] H. Niu, M. Gao, *Angew. Chem. Int. Ed.* **2006**, *45*, 6462.
[8] Y. Jin, X. Gao, *J. Am. Chem. Soc.* **2009**, *131*, 17774.
[9] Y. Yin, R. M. Rioux, C. K. Erdonmez, S. Hughes, G. A. Somorjai, A. P. Alivisatos, *Science* **2004**, *304*, 711.
[10] H. J. Fan, U. Gosele, M. Zacharias, *Small* **2007**, *3*, 1660.
[11] X. W. Lou, Y. Wang, C. Yuan, J. Y. Lee, L. A. Archer, *Adv. Mater.* **2006**, *18*, 2325.
[12] H. C. Zeng, *Curr. Nanosci.* **2007**, *3*, 177.
[13] H. G. Yang, H. C. Zeng, *J. Phys. Chem. B* **2004**, *108*, 3492.
[14] Y. G. Sun, B. T. Mayers, Y. N. Xia, *Nano Lett.* **2002**, *2*, 481.
[15] Y. D. Yin, C. Erdonmez, S. Aloni, A. P. Alivisatos, *J. Am. Chem. Soc.* **2006**, *128*, 12671.
[16] K. An, S. G. Kwon, M. Park, H. B. Na, S.-Il. Baik, J. H. Yu, D. Kim, J. S. Son, Y. W. Kim, I. C. Song, W. K. Moon, H. M. Park, T. Hyeon, *Nano Lett.* **2008**, *8*, 4252.
[17] Y. Xia, T. D. Nguyen, M. Yang, B. Lee, S. Aaron, P. Podsiadlo, Z. Tang, S. C. Glotzer, N. A. Kotov, *Nat. Nanotechnol.* **2011**, *6*, 580.
[18] A. E. Persson, B. J. Schoeman, J. Sterte, J. E. Otterstedt, *Zeolites* **1994**, *14*, 557.
[19] W. W. Yu, L. Qu, W. Guo, X. Peng, *Chem. Mater.* **2003**, *15*, 2854.
[20] J. J. Li, Y. A. Wang, W. Guo, J. C. Keay, T. D. Mishima, M. B. Johnson, X. Peng, *J. Am. Chem. Soc.* **2003**, *125*, 12567.
[21] L. Jiang, Y. Zhong, G. Li, *Mater. Res. Bull.* **2009**, *44*, 999.

[22] Q. Zhang, C. M. Cobley, J. Zeng, L. P. Wen, J. Chen, Y. Xia, *J. Phys. Chem. C* **2010**, *114*, 6396.
[23] D. Battaglia, B. Blackman, X. Peng, *J. Am. Chem. Soc.* **2005**, *127*, 10889.
[24] G. Hodes, *Chemical Solution Deposition of Semiconductor Films*. CRC Press, Boca Raton, FL **2002**, Ch. 4.
[25] A. Janeković, E. Matijević, *J. Colloid Interface Sci.* **1985**, *103*, 436.
[26] L. Liu, Q. Peng, Y. Li, *Inorg. Chem.* **2008**, *47*, 3182.
[27] L. Liu, Q. Peng, Y. Li, *Inorg. Chem.* **2008**, *47*, 5022.
[28] J. X. Huang, Y. Xie, B. Li, Y. Liu, Y. T. Qian, S. Y. Zhang, *Adv. Mater.* **2000**, *12*, 808.
[29] Y. R. Ma, L. M. Qi, J. M. Ma, H. M. Cheng, W. Shen, *Langmuir* **2003**, *19*, 9079.
[30] G. Lin, J. Zheng, R. Xu, *J. Phys. Chem. C* **2008**, *112*, 7363.
[31] Y. Wang, Z. Tang, M. A. Correa-Duarte, I. Pastoriza-Santos, M. Giersig, N. A. Kotov, L. M. Liz-Marzán, *J. Phys. Chem. B* **2004**, *108*, 15461.
[32] J. R. Lakowicz, *Principles of Fluorescence Spectroscopy*, 2nd ed., Kluwer Academic/Plenum Publishers, New York **1999**.
[33] D. V. Talapin, I. Mekis, S. Gotzinger, A. Kornowski, O. Benson, H. Weller, *J. Phys. Chem. B* **2004**, *108*, 18826.
[34] Y. Sun, B. Wiley, Z. Y. Li, Y. Xia, *J. Am. Chem. Soc.* **2004**, *126*, 9399.
[35] T. Zhang, J. Ge, Y. Hu, Q. Zhang, S. Aloni, Y. Yin, *Angew. Chem. Int. Ed.* **2008**, *47*, 5806.
[36] J. C. Park, H. Song, *Nano Res.* **2011**, *4*, 33.
[37] X. Huang, C. Guo, J. Zuo, N. Zheng, G. D. Stucky, *Small* **2009**, *5*, 361.
[38] Y. Zhu, T. Ikoma, N. Hanagata, S. Kaskel, *Small* **2010**, *6*, 471.
[39] Y. Lu, Y. Zhao, L. Yu, L. Dong, C. Shi, M. Hu, Y. Xu, L. Wen, S. H. Yu, *Adv. Mater.* **2010**, *22*, 1407.
[40] H. Liu, D. Chen, L. Li, T. Liu, L. Tan, X. Wu, F. Tang, *Angew. Chem. Int. Ed.* **2011**, *50*, 891.
[41] J. Liu, S. Z. Qiao, J. S. Chen, X. W. (D.) Lou, X. Xing, G. Q. (M.) Lu, *Chem. Commun.* **2011**, *47*, 12578.
[42] P. Mulvaney, *Langmuir* **1996**, *12*, 788.
[43] T. Mokari, E. Rothenberg, I. Popov, R. Costi, U. Banin, *Science* **2004**, *304*, 1787.
[44] R. Costi, A. E. Saunders, U. Banin, *Angew. Chem. Int. Ed.* **2010**, *49*, 4878.
[45] W. T. Chen, T. T. Yang, Y. J. Hsu, *Chem. Mater.* **2008**, *20*, 7204.
[46] Y. Jin, X. Gao, *Nat. Nanotechnol.* **2009**, *4*, 571.
[47] J. Turkevich, J. Hillier, P. C. Stevenson, *Discuss. Faraday Soc.* **1951**, *11*, 55.